

# The miR-181d-regulated metalloproteinase Adamts1 enzymatically impairs adipogenesis via ECM remodeling

S-Z Chen<sup>1,2</sup>, L-F Ning<sup>1,2</sup>, X Xu<sup>3</sup>, W-Y Jiang<sup>1,2</sup>, C Xing<sup>1,2</sup>, W-P Jia<sup>4,5</sup>, X-L Chen<sup>6</sup>, Q-Q Tang<sup>\*1,2,3</sup> and H-Y Huang<sup>\*1,2,3</sup>

The extracellular matrix (ECM) maintenance is crucial to the structural integrity of adipocytes and whole adipose tissue formation. However, the potential impact of the ECM on adipocyte lineage commitment is unclear. Herein, we demonstrate that forced expression of matrix-associated metalloproteinase Adamts1 (a disintegrin and metalloproteinase with thrombospondin motifs 1), which we show is targeted by microRNA-181d (miR-181d) during BMP4-induced adipocytic lineage commitment, markedly impairs adipocyte commitment. Conversely, siRNA-induced inhibition of Adamts1 promotes adipocyte commitment. Adamts1 metalloprotease activity is required for this inhibition and is determined to function via remodeling ECM components followed by activating FAK–ERK signaling pathway during the commitment process. Furthermore, ablation of Adamts1 in adipose tissue increases adipose tissue mass, reduces insulin sensitivity, and disrupts lipid homeostasis. This finding is consistent with Adamts1 decreased expression in the adipose tissue of obese mice and an inverse correlation of Adamts1 expression with body mass index in humans. Collectively, our results indicate that Adamts1 acts as an ECM ‘modifier’, with miR-181d-induced downregulation, that regulates adipocyte lineage commitment and obesity.

*Cell Death and Differentiation* (2016) 23, 1778–1791; doi:10.1038/cdd.2016.66; published online 22 July 2016

Obesity is characterized by adipose mass expansion through adipocyte hypertrophy and hyperplasia, followed by localized angiogenesis, inflammatory cell infiltration, and extracellular matrix (ECM) remodeling.<sup>1–3</sup> The protein composition and dynamics of the ECM are of crucial importance to adipocyte function.<sup>4</sup> Among the ECM proteins, collagens are the most abundant protein constituents of interstitial fibers and pericellular basement membranes.<sup>5</sup> Recent reports suggest that obese individuals display excess collagen deposition in adipose tissues.<sup>6,7</sup> Thbs1, another important ECM protein, has been characterized as an adipokine that is highly expressed in obese subjects.<sup>8</sup> Loss of Thbs1 expression attenuated weight gain and fat accumulation in high-fat diet (HFD) mice.<sup>9</sup> Fibronectin is also abundant in mature adipose tissue.<sup>10</sup> Moreover, other matrix components such as SPARC, osteopontin, decorin, and tenascin C increase significantly in white adipose tissue of obesity individuals.<sup>11–13</sup> These reports suggest that common ECM molecules provide a critical microenvironment that may impact adipocyte bioactivity and interaction with other cell types. However, few

molecular mechanisms for ECM protein regulation of adipogenesis have been defined.

As ECM function depends on its molecular composition, it is important to establish which proteins have been identified as ECM modifiers in adipose tissue. In fact, ECM remodeling requires a balance between constructive and destructive enzymes together with their enhancers and inhibitors.<sup>4</sup> Proteolytic matrix metalloproteases (MMPs) that degrade ECM and basement membrane components are required for adipose tissue development.<sup>14,15</sup> However, unlike MMPs, the presence and function of the protein Adamts (a disintegrin and metalloproteinase with thrombospondin motifs) in adipose tissue are not fully recognized.

The metalloprotease Adamts1 is characterized by three thrombospondin (TSP)-like domains located at its C terminus. This member of the Adamts extracellular proteases is involved in the processing of procollagen I, procollagen III, and proteoglycans.<sup>16,17</sup> Adamts1 is synthesized as a p<sup>110</sup> pro-zymogen form that undergoes N-linked glycosylation following protein translation followed by furin enzymatic cleavage to release a p<sup>87</sup> active form. The p<sup>87</sup> active protease can subsequently

<sup>1</sup>Department of Biochemistry and Molecular Biology, School of Basic Medical Sciences, Fudan University, Shanghai 200032, China; <sup>2</sup>Key Laboratory of Metabolism and Molecular Medicine, The Ministry of Education, China; <sup>3</sup>Institute of Stem Cell Research and Regenerative Medicine, Institutes of Biomedical Sciences, Fudan University, Shanghai 200032, China; <sup>4</sup>Department of Endocrinology and Metabolism, Shanghai Clinical Center for Diabetes, Shanghai Jiaotong University Affiliated Sixth People's Hospital, Shanghai 200233, China; <sup>5</sup>Shanghai Diabetes Institute, Shanghai Key Laboratory of Diabetes Mellitus, Shanghai 200233, China and <sup>6</sup>Department of Food Science and Nutrition, University of Minnesota-Twin Cities, Saint Paul, MN 55108, USA

\*Corresponding author: H-Y Huang or Q-Q Tang, Department of Biochemistry and Molecular Biology, School of Basic Medical Sciences, Fudan University or Key Laboratory of Metabolism and Molecular Medicine, The Ministry of Education, Room 513, 13# Building, 138 Yixueyuan Road, Shanghai 200032, China. Tel: +86 21 54237125; Fax: +86 21 64033738; E-mail: haiyanhuang@shmu.edu.cn or qqtang@shmu.edu.cn

**Abbreviations:** Adamts1, a disintegrin and metalloproteinase with thrombospondin motifs 1; ECM, extracellular matrix; BMI, body mass index; HFD, high-fat-diet; iWAT, inguinal white adipose tissue; eWAT, epididymal white adipose tissue; BAT, brown adipose tissue; SVF, stromal vascular fraction; MMPs, matrix metalloproteases; MSCs, mesenchymal stem cells; ERK1/2, extracellular signal-regulated kinases 1 and 2; FAK, focal adhesion kinase; BMP4, bone morphogenetic protein 4; Pref1, preadipocyte factor 1; PPAR $\gamma$ , peroxisome proliferator-activated receptor  $\gamma$ ; C/EBP $\alpha$ , CCAAT enhancer-binding protein  $\alpha$ ; 422/aP2, fatty acid-binding protein; GTT, glucose tolerance tests; ITT, insulin tolerance tests; LDL-C, low-density lipoprotein-cholesterol

Received 23.11.15; revised 09.5.16; accepted 13.6.16; Edited by G Melino; published online 22.7.2016

undergo a secondary processing event to release a p<sup>65</sup> active form that cleaves the last two TSP repeats mediated by MMP2, 8, and 15.<sup>18</sup> In general, Adamts1 has two types of biological functions based on its structure: the metalloprotease-dependent catalytic degradation of ECM components, such as cleavage of Thbs1, aggrecan, versican, syndecan-4, semaphorin 3C, and type I collagen;<sup>19–23</sup> and non-catalytic, TSP-dependent angiogenesis inhibition.<sup>24,25</sup> Of note, Adamts1 may also have other functions related to the inflammatory response.<sup>26</sup>

Adamts1 has been implicated in organogenesis, embryogenesis, wound repair, cancer development, and liver fibrosis.<sup>27–30</sup> However, the specific roles of Adamts1 in adipogenesis, which include mesenchymal stem cell (MSC) lineage commitment and their terminal differentiation into adipocytes, remain undefined. Here, we demonstrate that Adamts1 has a crucial role in adipocyte lineage commitment via ECM-dependent FAK-ERK signaling pathway. Furthermore, we show that Adamts1 knockdown in adipose tissue increases adipose tissue mass, reduces insulin sensitivity and disrupts lipid homeostasis. These observations are in agreement with the findings of decreased Adamts1 expression in the adipose tissue of obese mice and an inverse correlation of Adamts1 expression with body mass index (BMI) in humans.

## Results

**Obesity reduces the accumulation of Adamts1 in adipose tissue.** To gain insight into Adamts1 biological activity, we first examined its expression profile in a wide range of tissues of C57BL/6J mice. As shown in Figure 1a, Adamts1 was highly expressed in inguinal and epididymal white adipose tissue (iWAT and eWAT), suggesting the involvement of Adamts1 in adipogenesis. We then evaluated ADAMTS1 expression in human adipose tissues. As shown in Figures 1b and c, Adamts1 mRNA expression in both subcutaneous and visceral white adipose tissues was inversely correlated with BMI. Parallel results in mice adipose tissues revealed that Adamts1 was markedly downregulated in ob/ob, db/db, and HFD-fed mice as compared with controls (Figures 1d and e). These results suggested that reduced expression of Adamts1 was indispensable to the development of obesity. It should also be noted that the most abundant Adamts1 protein form in adipose tissue was p<sup>65</sup> (Supplementary Figure S1), so only the results for the p<sup>65</sup> form are presented for the following experiment. We next isolated the stromal vascular fraction (SVF) and mature adipocytes from the adipose tissue of both HFD-fed and normal chow-fed mice to determine the Adamts1 mRNA expression profile. Results showed that Adamts1 expression in both SVF and mature adipocytes was decreased in iWAT and eWAT from C57BL/6J mice on a HFD as compared with controls (Figure 1f). However, Adamts1 exhibited relatively higher transcription levels in SVF compared with the mature adipocyte, suggesting that Adamts1 might have a pivotal role in the process of MSC commitment to form preadipocytes.

**Adamts1 impairs BMP4-induced adipocyte lineage commitment.** As described previously,<sup>31</sup> BMP4 induces nearly complete commitment of C3H10T1/2 cells to the adipocyte

lineage. We next detected Adamts1 expression during BMP4-induced commitment of C3H10T1/2 cells (Supplementary Figure S2A). The results revealed that Adamts1 is negatively regulated by BMP4 treatment in a dose-dependent manner (Figures 2a and b; Supplementary Figure S2B). A more detailed trend in the change is illustrated in Figure 2c, with Adamts1 showing continuously lower protein expression under BMP4 treatment compared with controls. Adamts1 mRNA was maintained at a stable lower level in the BMP4-treated group, while it was continuously raised in controls (Figure 2d). The impact of BMP4 on Adamts1 was also confirmed in adipose tissue-specific BMP4 transgenic mice.<sup>32</sup> Adamts1 expression was significantly decreased in adipose tissue from BMP4 transgenic mice compared with genetically matched wild-type controls (Figures 2e and f; Supplementary Figure S2C). These results further confirmed that BMP4 could downregulate the expression of Adamts1. To characterize the function of Adamts1 in adipocyte lineage commitment, we first conducted an RNA interference experiment using specific siRNA to knockdown Adamts1 expression. Adamts1 expression was significantly reduced in both BMP4-treated cells and control cells as confirmed by western blot and qRT-PCR (Figures 2g and h; Supplementary Figure S2A). Adamts1 knockdown induced expression of preadipocyte factor 1 (Pref1), a preadipocyte marker protein, even in the absence of BMP4, suggesting more C3H10T1/2 MSCs were committed to preadipocytes (Figure 2g). Meanwhile, more mature adipocytes were acquired when cells were treated with a standard adipocyte differentiation protocol, as reflected by increased cytoplasmic triglyceride staining with Oil Red O (Figure 2i; Supplementary Figure S2D and E) and upregulation of adipocyte-specific marker proteins PPAR $\gamma$ , C/EBP $\alpha$ , and 422/aP2 (Figure 2j). Conversely, when Adamts1 was overexpressed in C3H10T1/2 cells using a retroviral system (MSCV), Pref1 expression was reduced with or without BMP4 treatment (Figures 2k and l; Supplementary Figure S2A). Adipogenesis was also inhibited in cells overexpressing Adamts1 (Figures 2m and n; Supplementary Figure S2F and G). These results suggested that Adamts1 impairs BMP4-induced adipocyte lineage commitment.

**Adamts1 protease activity is required to impair adipocyte lineage commitment.** The Adamts1 metalloproteinase catalytic site of the zinc-binding peptidase (HEXXHXXXXXHD) was conserved across various species (Figure 3a). Therefore, a point mutation E403Q, in which the essential Glu residue was converted to Gln, was introduced into the Adamts1 metalloproteinase catalytic domain to underscore the enzyme's role in regulating the adipocyte lineage commitment (Figure 3b). Inhibition of Pref1 expression by Adamts1 was reversed by this metalloproteinase mutation (Figure 3c). In addition, adipogenesis was also restored (Figures 3d and e; Supplementary Figure S3A and B). To explore Adamts1 substrates impacting adipocyte lineage commitment, expression of the ECM proteins Thbs1, Fibronectin, and collagens<sup>5,8–10</sup> were evaluated. These molecules were downregulated by Adamts1 overexpression with/out BMP4, but not by Adamts1 enzyme inactivation (Figure 3f). In contrast, Adamts1 silencing increased their expression in the

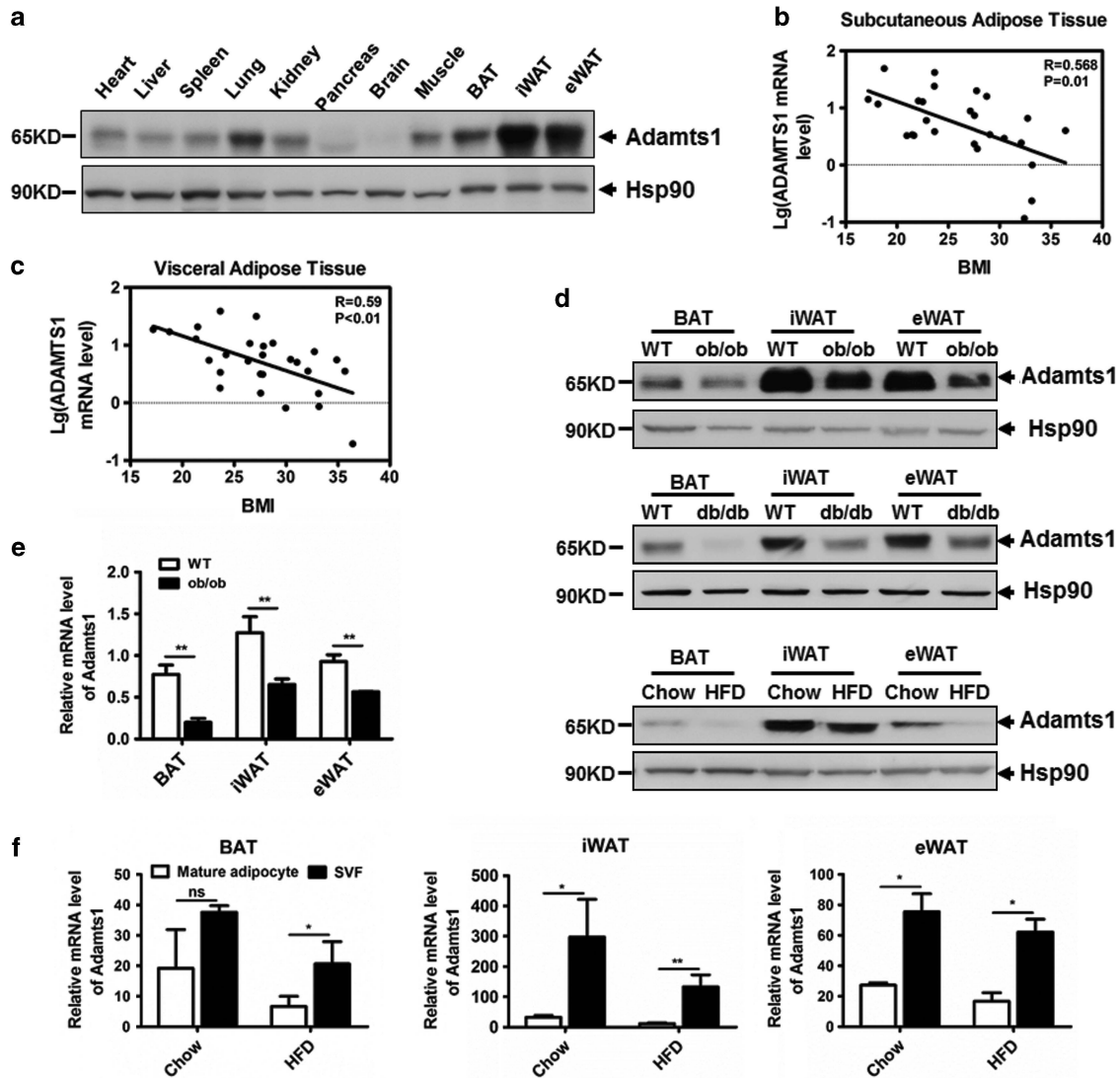


**Figure 1** Adamts1 expression level is decreased in obesity. (a) Adamts1 protein expression profile in C57BL/6J wild-type mouse tissues as detected by western blot. Heat shock protein (Hsp90) was used as a loading control. (b and c) Linear regression analysis of BMI and Adamts1 expression in human subcutaneous ( $n=28$ ) and visceral ( $n=29$ ) adipose tissue. (d) Western blot analysis of Adamts1 protein expression in interscapular brown adipose tissue (BAT), inguinal white adipose tissue (iWAT), and epididymal WAT (eWAT) from ob/ob, db/db, and high-fat diet (HFD)-fed mice. (e) qRT-PCR analysis of Adamts1 mRNA expressed in BAT, iWAT, and eWAT from wild-type and ob/ob mice ( $n=6$ ). (f) Adamts1 expression in mature adipocytes and the stromal vascular fraction from BAT, iWAT and eWAT that are from mice fed with normal chow or HFD ( $n=6$ ). qRT-PCR analysis of the fold change in Adamts1 expression normalized to endogenous 18S expression. Data are presented as the mean  $\pm$  S.E.M. \* $P<0.05$ , \*\* $P<0.01$

presence of BMP4 (Figure 3g). As a read-out of Adamts1 expression changes, the expression of Col5a1, Col1a1, and Thbs1 were evaluated in adipose tissues from mice and human. As shown in Supplementary Figure S3C–I, these molecules were upregulated in adipose tissue of HFD and ob/ob mice as compared with control mice. Similarly, mRNA level of these molecules in both subcutaneous and visceral adipose tissues were positively correlated with BMI, which suggesting an inverse correlation between these factors and Adamts1.

**FAK-ERK1/2 involves in Adamts1-mediated impairment of adipocyte lineage commitment.** To elucidate the mechanism underlying Adamts1-mediated impairment of adipocyte lineage commitment, the activity of potential signaling

pathways was evaluated. It has been reported that the p38/Smad signaling pathway is required for adipocyte lineage commitment.<sup>33</sup> Thus, we wondered whether Adamts1 might influence the p38/Smad signaling pathway. However, no obvious change was observed with overexpressing or silencing Adamts1 (Figures 4a and b). We next investigated the extracellular signal-regulated kinases 1 and 2 (ERK1/2) signaling pathway, which mediates the function of a variety of ECM proteins through integrin receptor signaling.<sup>34</sup> As illustrated in Figure 4a, overexpression of wild-type Adamts1 activated ERK1/2 signaling, while inactivated Adamts1 had no effect. Conversely, Adamts1 silencing markedly decreased ERK1/2 phosphorylation with/without BMP4 treatment (Figure 4b). It has been reported that association of focal adhesion kinase (FAK) with Src leads to activation of ERK via

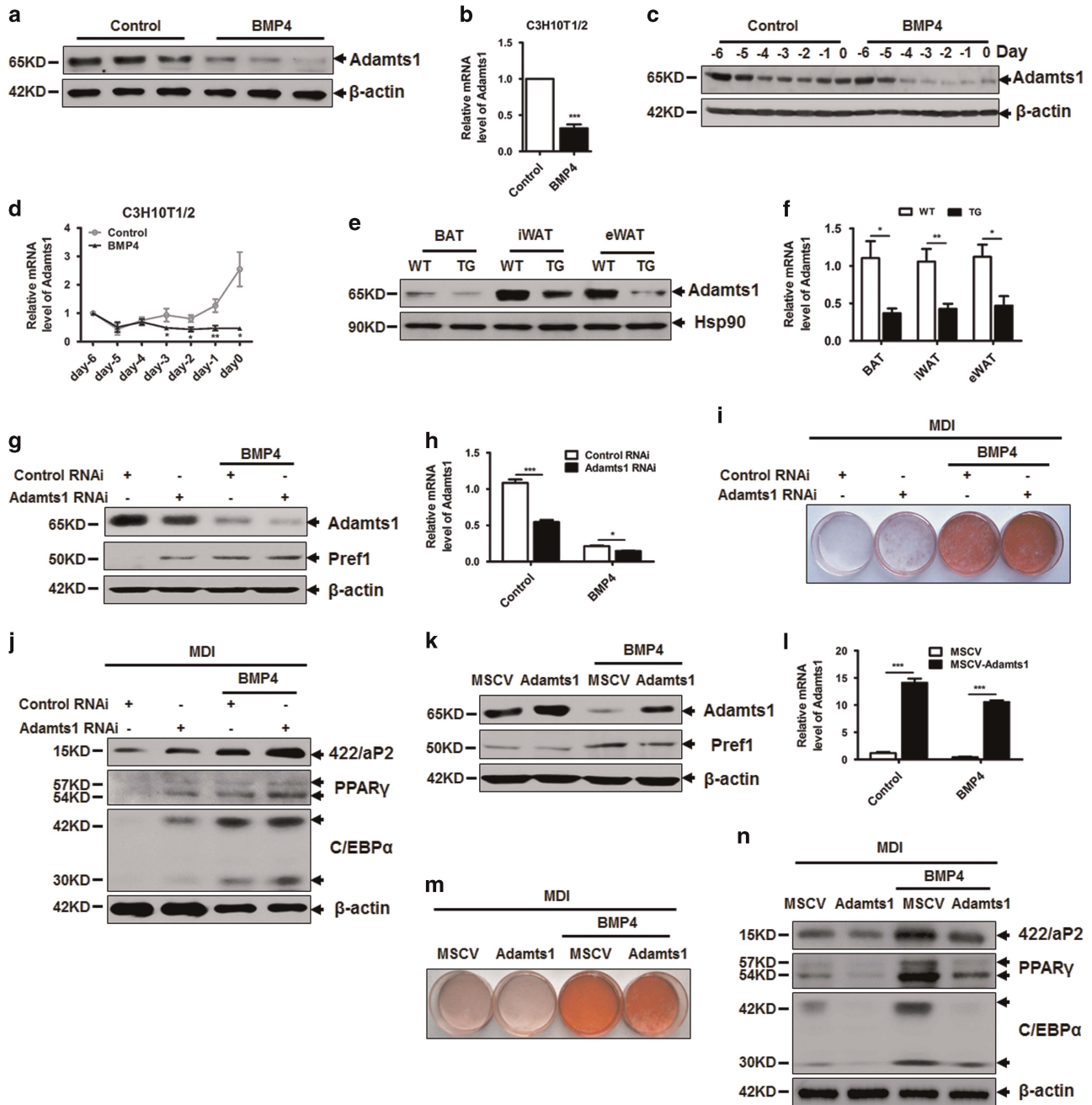


**Figure 2** Adamts1 inhibits the adipocyte lineage commitment of C3H10T1/2 cells. (a and b) Western blot and qRT-PCR detection of Adamts1 expression in BMP4-induced, committed preadipocytes. C3H10T1/2 cells were treated without or with BMP4 (20 ng/ml) until postconfluence, and then cell lysates were subjected to SDS-PAGE, or total RNA was isolated for qRT-PCR amplification. (c and d) Western blot and qRT-PCR detection of Adamts1 expression during C3H10T1/2 cell commitment. (e and f) Western blot and qRT-PCR detection of Adamts1 expression in BAT, iWAT, and eWAT from wild-type and BMP4 transgenic (TG) mice ( $n = 6$ ). (g) C3H10T1/2 cells were incubated with Adamts1 siRNA or negative control siRNA for 24 h prior to treatment without or with BMP4 (10 ng/ml). Cells were grown until postconfluence, and then cell lysates were subjected to SDS-PAGE. Western blots were probed with antibodies to Adamts1 or Pref1, with  $\beta$ -actin used as a loading control. (h) qRT-PCR was performed to determine Adamts1 mRNA expression. (i and j) After reaching postconfluence, cell differentiation was induced (MDI). The effects of Adamts1 silencing on adipocyte lineage commitment and subsequent differentiation were assessed at day 6 by Oil Red O staining and 422/aP2, C/EBP $\alpha$ , and PPAR $\gamma$  protein expression. (k) Retrovirus-infected C3H10T1/2 cells were treated without or with BMP4 (20 ng/ml) until postconfluence, and then cell lysates were subjected to SDS-PAGE. Western blots were probed with antibodies to Adamts1 or Pref1, with  $\beta$ -actin used as a loading control. (l) qRT-PCR was performed to determine Adamts1 mRNA expression. (m and n) Postconfluent cells were induced to differentiate (MDI). The effects of Adamts1 upregulation on adipocyte lineage commitment and subsequent differentiation were assessed at day 6 by Oil Red O staining and protein expression by Western blot. qRT-PCR analysis of the fold change in Adamts1 expression were normalized to endogenous 18S expression. Data are presented as the mean  $\pm$  S.E.M. \* $P < 0.05$ , \*\* $P < 0.01$ , \*\*\* $P < 0.001$ .

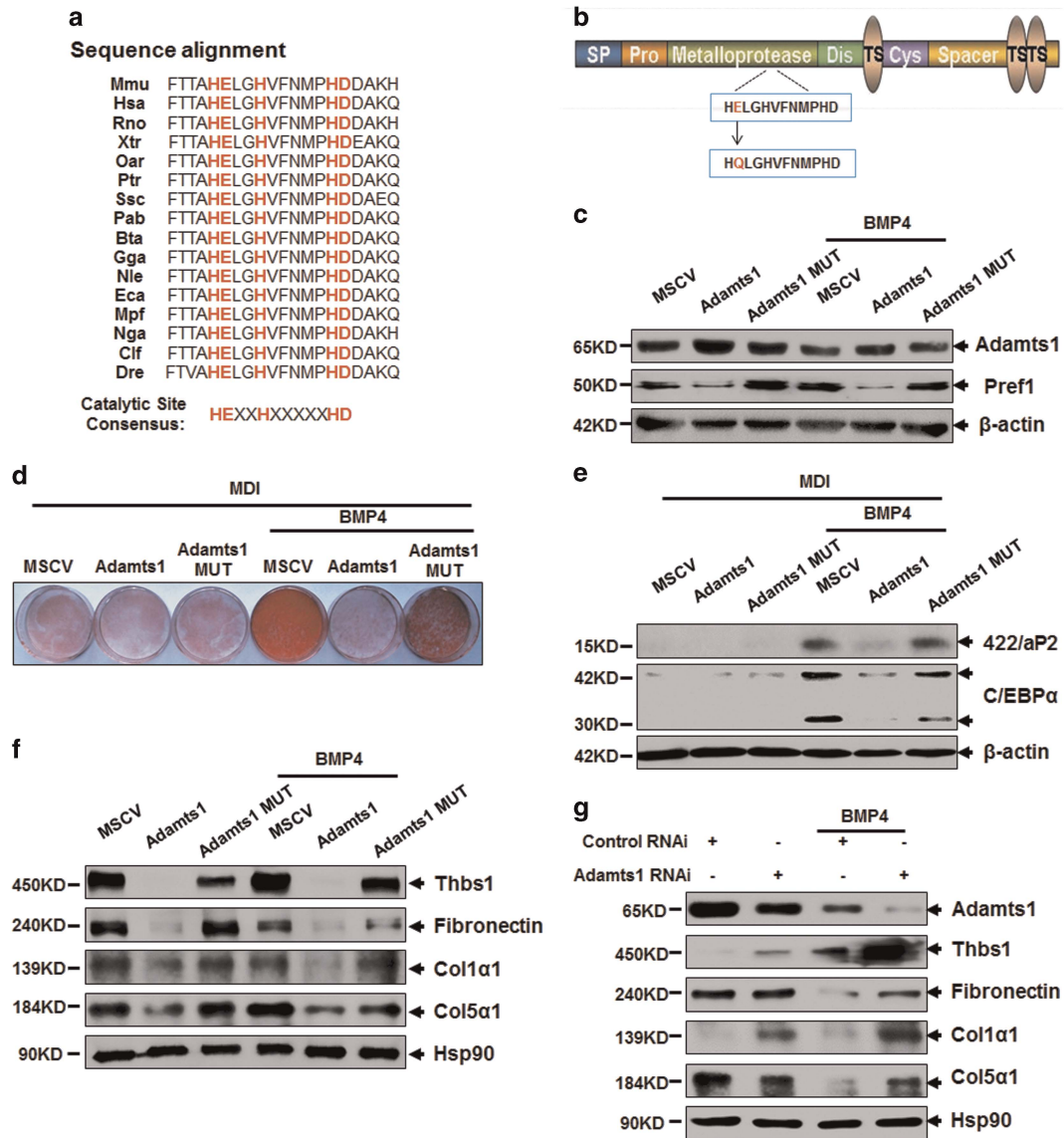


**Figure 3** Adamts1 enzymatically remodels the ECM during adipocyte lineage commitment. (a) Sequence alignment comparison of the residue in the Adamts1 metalloproteinase catalytic domain across various species. *Mmu* (house mouse), *Hsa* (human), *Rno* (Norway rat), *Xtr* (tropical clawed frog), *Oar* (sheep), *Ptr* (chimpanzee), *Ssc* (Pig), *Pab* (Sumatran orangutan), *Bta* (cattle), *Gga* (chicken), *Nle* (northern white-cheeked gibbon), *Eca* (horse), *Mpf* (domestic ferret), *Nga* (Upper Galilee mountains blind mole rat), *Cif* (dog), and *Dre* (zebrafish). (b) A point mutation, in which the essential Glu (E) residue was converted to Gln (Q), was conducted in the zinc ion binding region of the Adamts1 metalloproteinase catalytic domain. (c) Adamts1 and Pref1 expression. C3H10T1/2 cells were treated without or with BMP4 (20 ng/ml) until they reached postconfluence. Western blots were probed with antibodies to Adamts1 or Pref1, with β-actin used as a loading control. (d and e) After reaching postconfluence, cell differentiation was induced (MDI). The effects of the Adamts1 catalytic domain mutation on adipocyte lineage commitment and subsequent differentiation was assessed at day 7 by Oil Red O staining and 422/aP2 and C/EBPα protein expression. (f and g) Western blots of postconfluent cell lysates were probed with the indicated antibodies, with Hsp90 used as a loading control

the Grb2-Sos-Ras pathway.<sup>35,36</sup> We hypothesized that FAK signaling pathways may provide a link between activation of ERK1/2 and ECM. As expected, overexpression of wild-type but not inactivated Adamts1 enhanced FAK phosphorylation level, while Adamts1 silencing induced the opposite effect (Figures 4a and b). When treated with PD58059, a selective and reversible MEK-1 inhibitor which can reduce phospho-ERK1/2 (Figures 4c–f), adipocyte lineage commitment was promoted as shown in Figures 4d, e, g and h and Supplementary Figure S4A–D. Meanwhile, PD98059 could accelerate the increase in Adamts1 silencing-induced

adipogenesis (Figures 4c–e; Supplementary Figure S4A and B). Moreover, PD98059 could also reverse the adipogenesis impairment by Adamts1 overexpression (Figures 4f–h; Supplementary Figure S4C and D). We also evaluated the feedback influence of ERK inhibition on Adamts1 downstream targets. However, no significant change was found as shown in Supplementary Figure S4E, further indicating that ERK is the downstream of these ECM proteins. Consequently, these results indicated that FAK-ERK1/2 signaling pathway is responsible for Adamts1-mediated impairment of BMP4-induced adipocyte lineage commitment.

**Disruption of Adamts1 expression in inguinal adipose tissue increases adipose tissue mass and impairs obesity-related metabolic homeostasis.** To test Adamts1's

function during *in vivo* adipogenesis, a recombinant adenovirus expressing Adamts1 short hairpin RNA (shRNA) was injected subcutaneously adjacent to one inguinal fat pad site

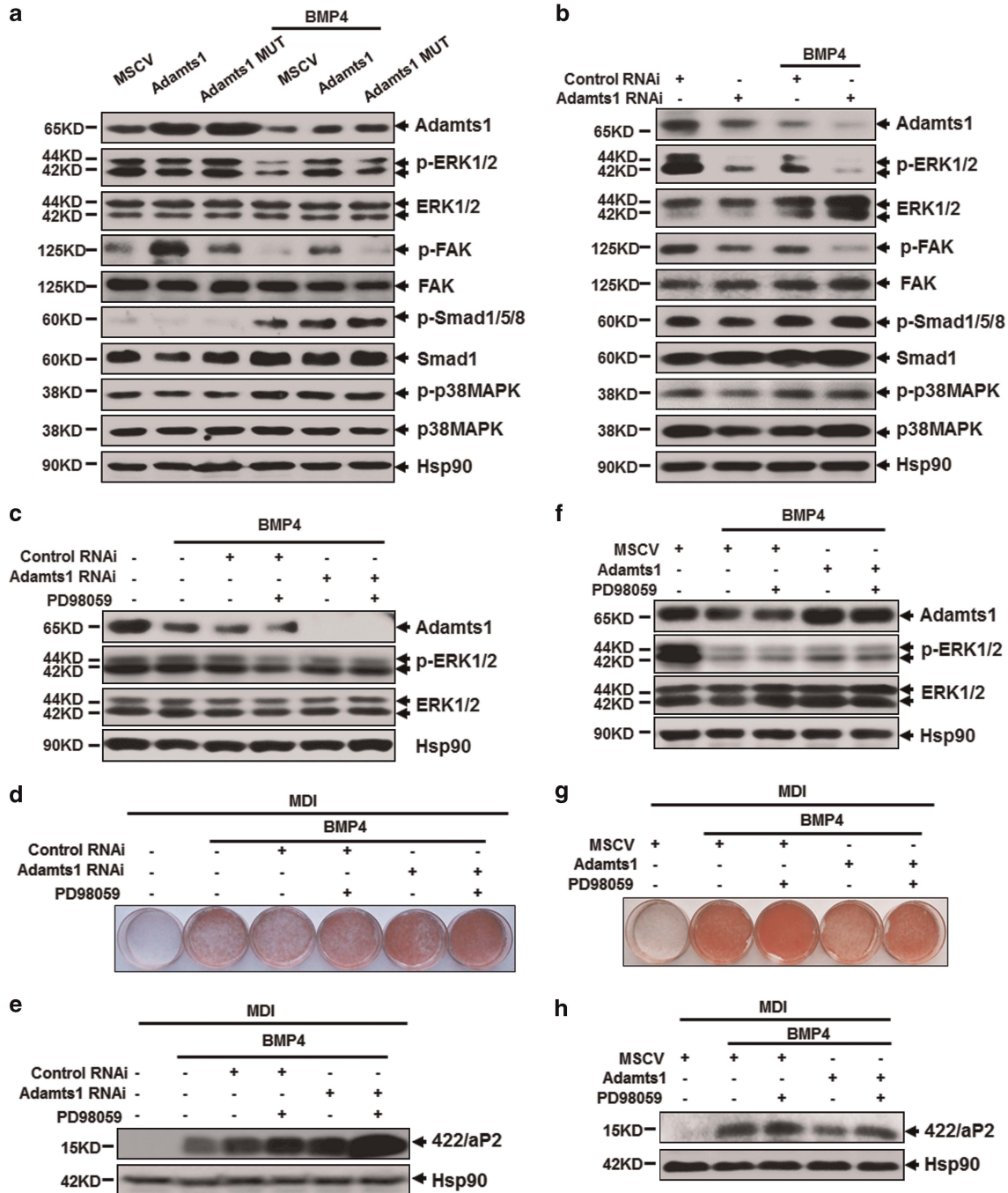


**Figure 4** Adamts1 activates the FAK-ERK1/2 signaling pathway during adipocyte lineage commitment. (a and b) C3H10T1/2 cells with Adamts1 overexpression or knockdown were treated without or with BMP4 (20 ng/ml). Western blots of postconfluent cell lysates were probed with the indicated antibodies, with Hsp90 used as a loading control. (c–e) C3H10T1/2 cells with Adamts1 knockdown were challenged with the ERK1/2 inhibitor PD98059 (25  $\mu$ M) 12 h prior to incubation with BMP4 (5 ng/ml). Western blots of postconfluent cell lysates were probed with the indicated antibodies, with Hsp90 used as a loading control (c). After reaching postconfluence, cell differentiation was induced (MDI). The effects of PD98059 on adipocyte lineage commitment and subsequent differentiation were assessed at day 6 by Oil Red O staining and 422/aP2 protein expression. Hsp90 was used as a loading control (d and e). (f–h) C3H10T1/2 cells with Adamts1 overexpression were challenged with the ERK1/2 inhibitor PD98059 (25  $\mu$ M) 12 h prior to incubation with BMP4 (20 ng/ml). Western blots of postconfluent cell lysates were probed with the indicated antibodies, with Hsp90 used as a loading control (f). After reaching postconfluence, cell differentiation was induced (MDI). The effects of PD98059 on adipocyte lineage commitment and subsequent differentiation were assessed at day 6 by Oil Red O staining and 422/aP2 protein expression. Hsp90 was used as a loading control (g and h)

in C57BL/6J mice, while recombinant adenovirus expressing LacZ shRNA was injected into the contralateral site as a control. The adeno-*Adamts1*-shRNA injection significantly decreased adipose *Adamts1* mRNA and protein expression compared with the contralateral control (Figures 5a and b). An expansion of iWAT was observed by *Adamts1* silencing (Figures 5c and d). The size of fat cells can be directly observed in hematoxylin and eosin (H&E) staining (Figure 5e) and be quantified by using Image J software (Figure 5f). By this way, enlargement of fat cell was observed with *Adamts1* knockdown compared with the paired contralateral LacZ shRNA control (Figures 5c–f), suggesting enhanced adipogenesis by *Adamts1* silencing. To further determine the impact of *Adamts1* silencing on whole-body metabolism, mice were subcutaneously injected with adeno-*Adamts1* shRNA adjacent to both inguinal fat pad sites and control mice were bilaterally injected with adeno-LacZ shRNA. Both groups were fed with normal chow diet or HFD, but group body weights diverged following adenovirus injection, with the *Adamts1* knockdown mice gaining more weight than the shLacZ control mice (Figure 5g). Accordingly, the inguinal fat pads with *Adamts1* knockdown showed obvious enlargement, but no difference was observed in the epididymal and interscapular fat pads or the liver (Supplementary Figure S5A–C). In addition, mice bilaterally injected with adeno-*Adamts1* shRNA exhibited higher fasting and random serum glucose than control mice (Figure 5h). Impaired insulin sensitivity and glucose tolerance were also observed in mice bilaterally injected with adeno-*Adamts1*-shRNA (Figures 5i and j). Moreover, lipid metabolism was also disrupted in mice with *Adamts1* silencing, as shown by elevations in plasma total cholesterol and low-density lipoprotein cholesterol (LDL-C) (Figure 5k). These results indicated that disruption of *Adamts1* expression in iWAT increased adipose tissue mass and impaired obesity-related metabolic homeostasis such as glucose and lipid metabolism.

**MiR-181d was identified as a putative upstream regulator of *Adamts1*.** We next sought to elucidate the mechanism of *Adamts1* regulation. Previous studies showed that the 3'-UTR of *Adamts1* affects its mRNA stability.<sup>37</sup> As *Adamts1* protein levels did not match its mRNA levels over the course of adipocyte lineage commitment (Figures 2c and d), we assessed possibility that *Adamts1* was regulated by microRNAs. Computational prediction of microRNAs targeting *Adamts1* was performed using the DIANA MICROT, MIRNA.ORG, and miRDB databases, and microRNA-181d (miR-181d) was identified as a putative upstream regulator of *Adamts1* across these three algorithms (Supplementary Figure S6A). Sequence analysis revealed that the 3'-UTR of *Adamts1* from various species was broadly conserved and that two putative binding sites within its 3'-UTR matched the seed sequence of miR-181d (Supplementary Figure S6A and B). To experimentally validate this potential target, the putative miR-181d-binding site and a mutated *Adamts1* 3'-UTR were, respectively, cloned into the psiCHECK2 vector and co-transfected with the miR-181d mimic or a negative control (Figure 6a). The miR-181d mimic significantly decreased wild-type *Adamts1* 3'-UTR luciferase activity, but had a minimal effect on the mutated *Adamts1* 3'-UTR reporter

luciferase activity (Figure 6b). In addition, *Adamts1* expression was inversely correlated with miR-181d expression in subcutaneous and visceral adipose tissues from human with different BMI and mice of HFD, ob/ob, and BMP4-TG (Figures 6c–g). Upregulation of miR-181d was also observed during the BMP4-treated adipocyte lineage commitment of C3H10T1/2 cells with reduced *Adamts1* expression (Figure 6h; Figures 2a–d; Supplementary Figure S6C). Then, we sought to explore whether a direct link exist between BMP4 and miR-181d expression. Our previous study reported that BMP/Smad signaling pathway has a dominant role in adipocyte lineage determination.<sup>33</sup> Interestingly, four SMAD-binding elements (SBEs) were found in the promoter of *miR-181d* gene. Thus, luciferase assay was performed to evaluate the impact of BMP4 on the SBEs activity of miR-181d promoter. The data suggested that the luciferase activity of wild-type miR-181d promoter was activated by BMP4, while luciferase activity of miR-181d promoter with SBE-deficient was unchanged (Figure 6i). These results indicated that BMP4-regulated miR-181d targeted *Adamts1* during adipogenesis.

**MiR-181d regulates *Adamts1*-ECM-FAK-ERK axis during BMP4-induced adipocyte lineage commitment.** To demonstrate the effect of miR-181d on *Adamts1* regulation, both retrovirus-miR-181d and specific inhibitor were used to verify the miR-181d function. As expected, overexpression of miR-181d in C3H10T1/2 cells resulted in reduced *Adamts1* expression (Figure 7a; Supplementary Figure S7A and B). In addition, adipogenesis was also promoted by overexpression of miR-181d, but were impaired by *Adamts1* co-overexpression (Figures 7a–c; Supplementary Figure S7C and D). Conversely, miR-181d inhibitor could increase the endogenous level of *Adamts1* and impair adipogenesis, while *Adamts1* silencing could rescue these effects (Figures 7d–f; Supplementary Figure S7E–G). These results revealed that miR-181d promotes adipogenesis by downregulating *Adamts1*. As a mediate of *Adamts1*'s function, ECM proteins and FAK-ERK pathway have also been assessed in miR-181d-*Adamts1* axis. Accordingly, miR-181d overexpression increased the expression of Thbs1, Fibronectin, Col1a1, and Col5a1, while co-overexpression of *Adamts1* reversed this pattern (Figure 7g). Afterwards, overexpression of miR-181d weakened FAK-ERK but not p38/Smad signaling pathway (Figure 7h). What's more, co-overexpression of *Adamts1* reversed this effect (Figures 7g and h). Correspondingly, miR-181d inhibitor reduced ECM protein level followed by activating the phosphorylation of FAK-ERK but not p38/Smad signaling pathway, while *Adamts1* silencing reversed this pattern (Figures 7i and j). Therefore, our results indicated that miR-181d promotes adipogenesis via targeting *Adamts1* followed by activation of ECM-FAK-ERK pathway.

## Discussion

In adipose tissues, mature adipocytes and their progenitor cells (preadipocytes) exist within an environment rich in ECM proteins.<sup>4,10,38</sup> The function of adipose tissue is regulated by physiological interactions between cells and ECM

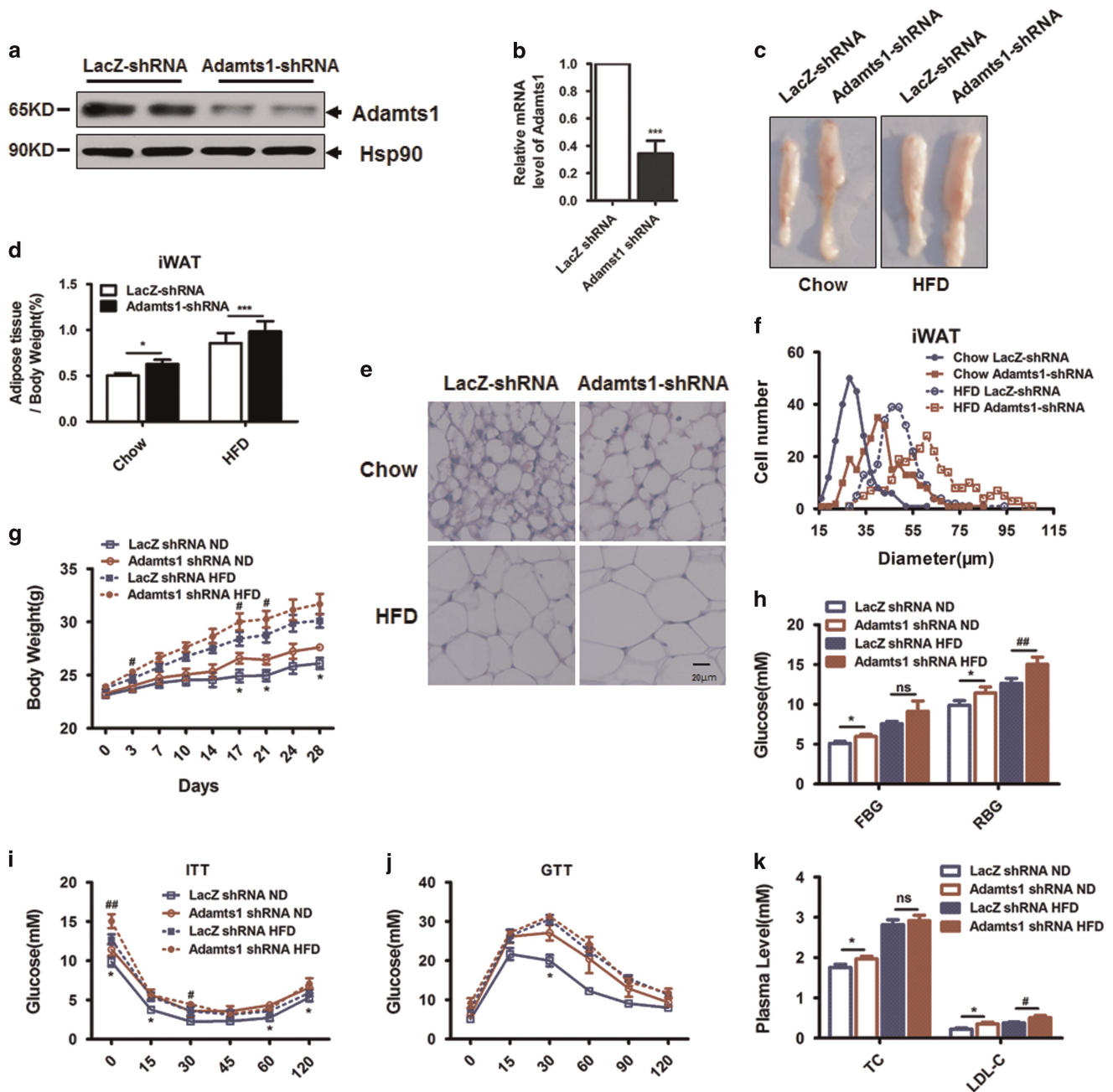


**Figure 5** Disruption of Adamts1 expression in inguinal adipose tissue promotes adipogenesis *in vivo*. (a–f) A recombinant adenovirus expressing Adamts1 shRNA was injected subcutaneously adjacent to one inguinal fat pad site. As a control, a recombinant adenovirus expressing LacZ shRNA was injected into the contralateral site. Mice were maintained on normal chow or HFD. (a and b) Western blot and qRT-PCR were used to detect Adamts1 expression in iWAT ( $n=5$ ). (c) Comparison of iWAT between fat pads. (d) iWAT fat index (percentage of fat pad weight relative to the whole body weight) ( $n=5$ ). (e) H&E staining of iWAT (Scale bar: 20  $\mu\text{m}$ ). (f) Quantification of iWAT adipocyte diameter. Image J software was used to collect data from H&E stained sections from 5 individual mice, 5 fields per mouse, 10–15 cells per field in each group. (g–k) C57BL/6J mice maintained on chow or HFD were injected subcutaneously adjacent to both inguinal fat pad sites with adeno-Adamts1 shRNA, while controls were injected with adeno-LacZ shRNA. (g) Body weight gain trends for injected mice ( $n=5$ ). (h) Fasting blood glucose (FBG) and random blood glucose (RBG) ( $n=5$ ) in mice. Glucose concentrations during an insulin tolerance test ( $n=5$ ) (i) or an i.p. glucose tolerance test ( $n=5$ ) (j). (k) Plasma total cholesterol and low-density lipoprotein-cholesterol (LDL-C) of injected mice

proteins.<sup>4,39,40</sup> Adipocyte differentiation requires space expansion, which stems from ECM remodeling.<sup>4,38</sup> ECM remodeling is regulated by a variety of modifiers, together with their respective enhancers and inhibitors. The Adamts proteins have been shown to contribute to proteolytic processes in the

ECM, with Adamts1, the first identified Adamts family member, able to cleave proteoglycan, aggrecan, collagen, elastin, and other ECM proteins.<sup>16,17,19</sup>

The results of the present study demonstrate that Adamts1 is crucial for adipose tissue development, and in



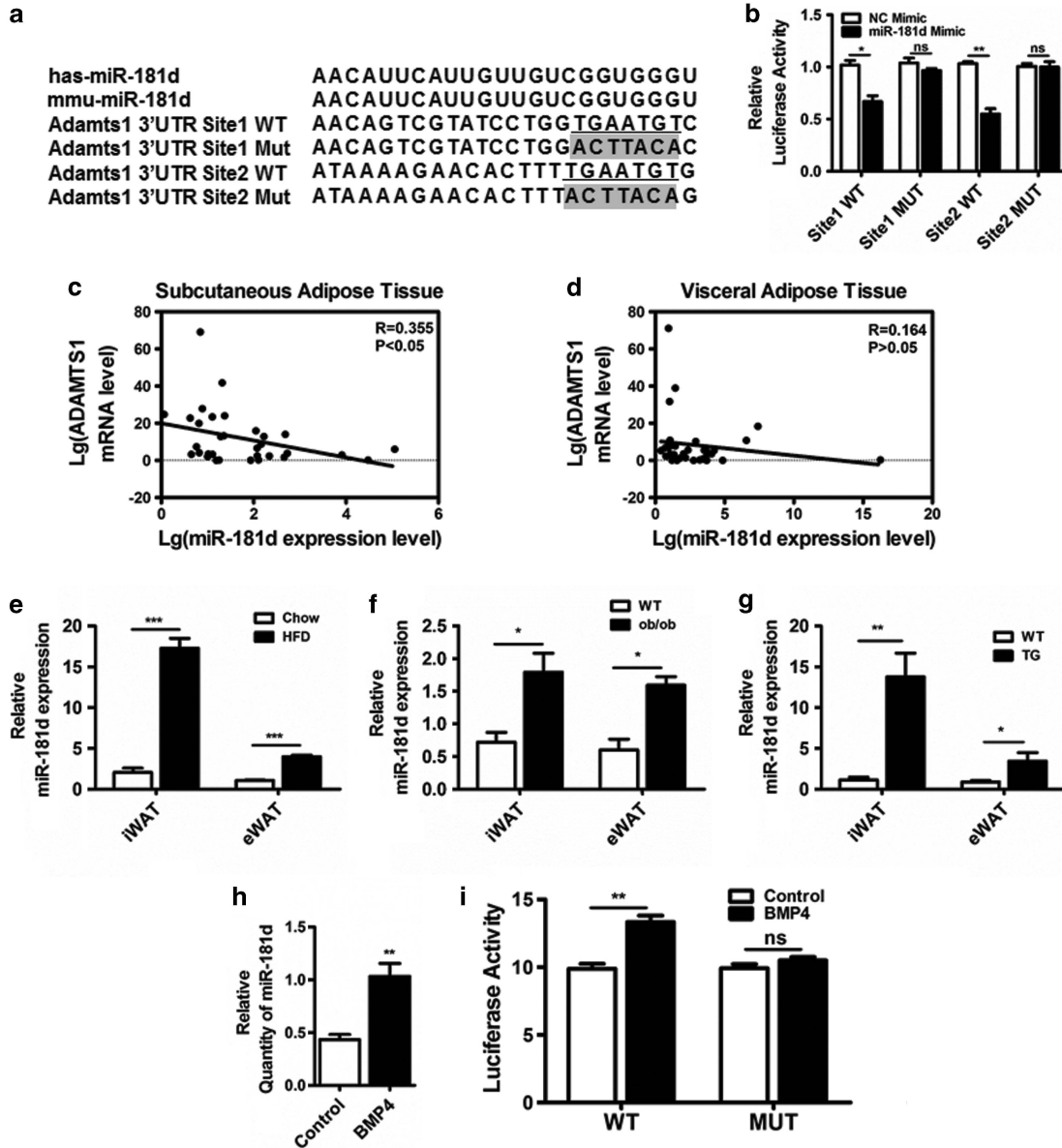
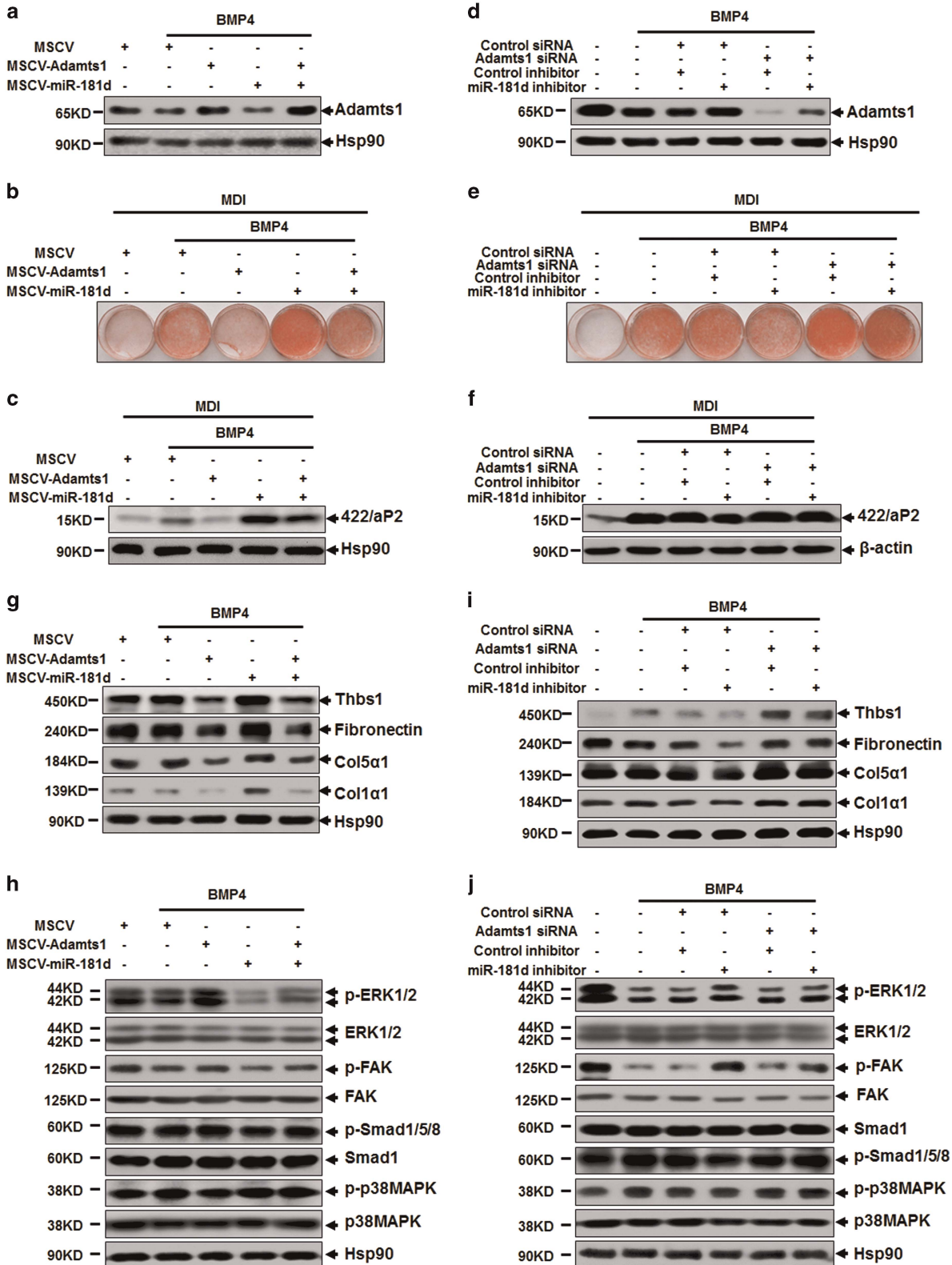


**Figure 6** *Adamts1* is targeted by miR-181d. (a) Schematic representation of miR-181d and *Adamts1* 3'-UTR. The seed sequence is underlined and the fonts with gray background indicate the nucleotides mutated in the *Adamts1* 3'-UTR. (b) Luciferase activity was determined using luminometry. 293T cells were transfected with 10 ng of mock psiCHECK2, psiCHECK2-*Adamts1* 3'-UTR-WT, or psiCHECK2-*Adamts1* 3'-UTR-Mut vector, plus 30 nM miR-181d mimic or a negative control mimic. Firefly and Renilla luciferase activities were measured in cell lysates, and values were normalized to the psiCHECK2 vector. Results are presented as fold change. (c and d) Linear regression analysis between *ADAMTS1* and miR-181d expression levels in human subcutaneous adipose tissues ( $n=30$ ) and visceral adipose tissues ( $n=30$ ). (e–g) The miR-181d expression in iWAT and eWAT from HFD ( $n=6$ ), *ob/ob* ( $n=6$ ), and BMP4 transgenic ( $n=6$ ) mice were detected using qRT-PCR. (h) qRT-PCR was performed to detect miR-181d expression in C3H10T1/2 cells on day 0. (i) Luciferase activity was determined using luminometry. 293T cells were transfected with 200 ng of mock psiCHECK2, psiCHECK2-miR-181d promoter-SBE-WT, or psiCHECK2-miR-181d promoter-SBE-MUT vector, plus 20 ng/ml BMP4 or control. Firefly and Renilla luciferase activities were measured in cell lysates, and values were normalized to the psiCHECK2 vector. Results are presented as the mean  $\pm$  S.E.M. \* $P<0.05$ , \*\* $P<0.01$ , \*\*\* $P<0.001$

**Figure 7** MiR-181d regulates the *Adamts1*-ECM-FAK-ERK axis. (a) C3H10T1/2 cells infected with MSCV-miR-181d or/and MSCV-*Adamts1* were treated with BMP4 (10 ng/ml) until postconfluent, cell lysis were subjected to SDS-PAGE to analyze the *Adamts1* protein expression, with Hsp90 as a loading control. (b and c) After reaching postconfluence, the cells were induced to differentiate into adipocytes (MDI). The effects of miR-181d or/and *Adamts1* overexpression on adipocyte lineage commitment and subsequent differentiation were assessed at day 6 by Oil Red O staining and 422/aP2 protein expression. (d) C3H10T1/2 cells incubated with miR-181d inhibitor or/and *Adamts1* siRNA were treated with BMP4 (10 ng/ml) until postconfluent, cell lysis were subjected to SDS-PAGE to analyze the *Adamts1* protein expression, with Hsp90 as a loading control. (e and f) After reaching postconfluence, the cells were induced to differentiate into adipocytes (MDI). The effects of miR-181d inhibitor or/and *Adamts1* siRNA on adipocyte lineage commitment and subsequent differentiation were assessed at day 6 by Oil Red O staining and 422/aP2 protein expression. (g–j) Western blots of postconfluent cell lysates were probed with the indicated antibodies, with Hsp90 used as a loading control

particular adipocyte lineage commitment. Forced expression of Adamts1 markedly impaired adipocyte lineage commitment, while siRNA-induced Adamts1 inhibition promoted the

commitment (Figure 2). *In vivo*, specific ablation of Adamts1 in iWAT enlarged the adipose mass and increased body weight (Figure 5). These results contradict previous reports



that Adamts1<sup>-/-</sup> mice display stunted growth and exhibit exceptionally lean bodies, together with a significantly reduced eWAT volume.<sup>28</sup> However, as Adamts1 is expressed in a number of tissues (Figure 1), it cannot be excluded that the change of fat in systemic knockout of Adamts1 may be caused by change in other tissues. However, in our model, selective disruption of Adamts1 resulted in iWAT fat pad enlargement, which provides more direct evidence between Adamts1 and adipose tissue. Surprisingly, Adamts1 disruption in iWAT impaired insulin sensitivity and plasma lipid homeostasis, indicating that Adamts1 involves in not only obesity but also obesity-related metabolic syndrome.

It is well established that adipocytes are enmeshed in a dense network of ECM.<sup>4,38</sup> The ECM components in adipose tissue are known to be regulated by matrix metalloproteinases and thereby enabled remodeling.<sup>41</sup> Thus, a concrete understanding of the biological functions of Adamts1, which can degrade varieties of substrates, will likely involve insights derived from identifying its substrates and regulation of its catalytic function. A point mutation within the Adamts1 zinc-binding motif eliminated its capacity to inhibit adipogenesis and to induce ECM remodeling (Figure 3), suggesting that Adamts1 catalytic function is critical in this process. The ECM contains many different proteins, such as Thbs1, Fibronectin, and collagens. During obesity, ECM protein expression is modified in WAT. In this study, we revealed that forced expression of Adamts1 nearly eliminates Thbs1 and Fibronectin expression. In addition, Adamts1 also catalyzes the degradation of typical fibril-forming collagens such as Col1 $\alpha$ 1 and Col5 $\alpha$ 1, which have been defined as a 'high-iWAT expression type'.<sup>10</sup> Moreover, the expression level of these ECM proteins were positively correlated with obesity, which further support a functional role of Adamts1 during adipogenesis (Supplementary Figure S3). It should be noted that the regulation of ECM is a complex systematic process involving a large number of molecules. Herein, we only concentrated on the regulation of Thbs1, Fibronectin and collagens during adipogenesis. However, other molecule like SPARC, which functions as an inhibitor of adipogenesis,<sup>42,43</sup> may also serve as a substrate of Adamts1 during adipocyte lineage commitment. Altogether, we propose that Adamts1 impairs adipocyte lineage commitment by influencing the cell microenvironment through degrading ECM components rather than regulating a single target or substrate.

The commitment of multipotent mesenchymal cells to various lineage types is determined by cytokine/growth factor stimuli and mechanical stresses transmitted by cell interactions with various ECM components that provide a structure for peripheral cells.<sup>34,38</sup> ECM changes initiate integrin signaling, altering intracellular microtubule and actin cytoskeletons and subsequently a cascade of downstream chemical events,<sup>44</sup> depending on the density of exposed integrin-binding sites.<sup>34</sup> Besides, cytoskeleton reorganization ultimately dictates the fate of multipotent mesenchymal cells.<sup>45</sup> Engagement of integrin  $\alpha$ 1 $\beta$ 1 and  $\alpha$ 2 $\beta$ 1 binding sites strongly activates ERK and impairs adipogenesis, while the engagement of  $\alpha$ v $\beta$ 3 binding sites strongly activates p38 kinase, which suppresses ERK in MSCs.<sup>34</sup> We have previously shown that p38/Smad signaling is required for adipocyte lineage commitment.<sup>33</sup> However, Adamts1 had no obvious influence

on p38/Smad in this study (Figure 4). In contrast, Adamts1 increased ERK1/2 phosphorylation during BMP4-mediated commitment of C3H10T1/2 cells, which agrees with other evidence that ERK activity is attenuated by BMP4 in embryonic stem cells.<sup>46</sup> Therefore, our findings suggest that Adamts1-induced microenvironment changes trigger the downstream ERK1/2 pathway. We then sought to answer the question why a metalloprotease-mediated ECM remodeling can affect the phosphorylation level ERK1/2. FAK locates closely with surface integrin receptors, which serve as a junction between cell and ECM.<sup>36</sup> The integrin engagement with ECM remodeling increased FAK tyrosine phosphorylation, which leads to activation of ERK1/2.<sup>35,36</sup> Indeed, our data verified that FAK signaling pathways provide a link between the activation of ERK1/2 and ECM remodeling during the adipocyte lineage commitment. Overall, FAK-activated ERK1/2 signaling pathway is responsible for Adamts1-mediated impairment of BMP4-induced adipocyte lineage commitment.

The miR-181 family were highly enriched in eWAT and reported to be important for the development and production of the pro-inflammatory B and T cells.<sup>47,48</sup> The TLR/NF $\kappa$ B-related miR-181a decreased in monocytes of obese individuals and is a putative biomarker of metabolic syndrome.<sup>49</sup> Moreover, miR-181a could promote adipogenesis via targeting TNF $\alpha$ ,<sup>50</sup> and downregulation of miR-181a could improve hepatic insulin sensitivity by upregulating sirtuin-1.<sup>51</sup> In this study, miR-181d was predicted to be a putative regulator of Adamts1. Interestingly, miR-181d has been reported to have a general role in regulating lipid content of hepatocytes via targeting Adamts5, which functions similarly with Adamts1.<sup>52</sup> Besides, miR-181d shares the same seed sequence with miR-181a, in view of which we supposed that miR-181d might participate in adipogenesis by targeting Adamts1. Our data confirmed that miR-181d promotes adipocyte lineage commitment by regulating Adamts1-ECM-FAK-ERK axis. Thus, we put forward for the first time that miR-181d is involved in adipogenesis and that its expression is strongly correlated with obesity.

In summary, this study has identified Adamts1 as a target of miR-181d that negatively regulates adipogenesis by impairing BMP4-induced adipocyte lineage commitment. The critical role of Adamts1 in this process is mediated through ECM remodeling that requires Adamts1 catalytic activity and followed by activating FAK-ERK1/2 pathway. These results provide new evidence regarding the role of Adamts1 in obesity and advance our understanding of the mechanistic regulation of adipocyte lineage commitment (Figure 8).

## Materials and Methods

**Human adipose tissue samples.** Pair of subcutaneous and visceral adipose tissues samples were collected from 30 patients who underwent metabolism-irrelevant surgeries at the Shanghai Sixth or Ninth People's Hospital, Shanghai JiaoTong University School of Medicine. Written informed consent to participate in this study was obtained from each patient. Patients ranged in age from 24 to 62 years old, and BMIs ranged from 17 to 49 kg/m<sup>2</sup>. This study was approved by the Ethics Committee of Shanghai Medical College, Fudan University and was conducted in accordance with the principles of the Helsinki Declaration II.

**Animal study.** Adipose tissue-specific BMP4 transgenic mice were generated as described before.<sup>32</sup> To build a mouse model of obesity, C57BL/6J mice were fed with HFD (51% kcal in fat, beginning at age 6 weeks) for 2.5 months and mice fed

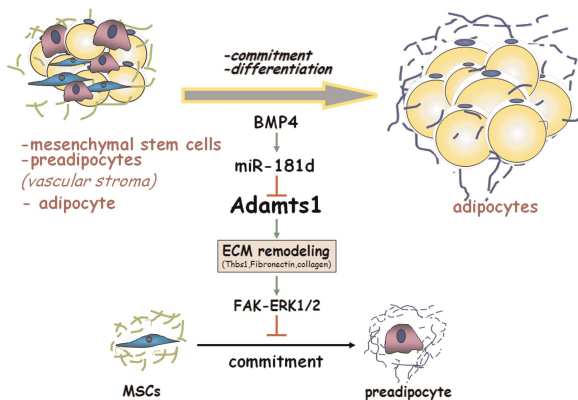


**Figure 8** Model of *Adams1*-mediated impairment of MSCs adipocyte commitment. Adipogenesis is a bi-phasic process: lineage commitment into preadipocytes, and terminal differentiation into mature adipocytes. *Adams1* is predominantly implicated in adipocyte lineage commitment and contributes to the development of obesity. *Adams1* impairs adipocyte lineage commitment through ECM remodeling following by activating FAK-ERK signaling pathway. Additionally, miR-181d, upregulated by BMP4, dominated *Adams1*-ECM-FAK-ERK axis during adipocyte lineage commitment

with normal chow diet were used as controls. All studies involving animal experimentation were approved by the Animal Experimental Ethics Committee of Shanghai Medical College, Fudan University, and followed the National Institute of Health guidelines on the care and use of animals.

#### Isolation of adipocytes and SVF from whole adipose tissue.

Adipocyte and SVF were isolated from adipose tissue of HFD and chow-fed C57BL/6J mice. Briefly, the adipose tissue was digested with an equal volume of collagenase type VIII (Sigma-Aldrich, St. Louis, MO, USA) containing 1% BSA for 1 h at 37 °C with shaking. Following complete digestion, the adipocytes were separated from the SVF by centrifugation at 1500 × *g* for 5 min. The floating adipocytes were transferred to a fresh tube, and the precipitated material containing SVF was resuspended with ammonium chloride lysis buffer to remove red blood cells.

**Plasmids and viral vectors.** Full-length mouse complementary DNA sequence for *Adams1* was amplified and subsequently cloned into the pMSCV-puro retroviral vector (Stratagene, Santa Clara, CA, USA). Likewise, the mmu-miR-181d precursor sequence was amplified from the mouse genome sequence and then cloned into pMSCV-puro retroviral vector.

Two fragments of the *Adams1* 3'-UTR, each containing a putative binding site or mutated site for miR-181d, were respectively cloned between the *Xho*I (5'-end) and *Not*I (3'-end) restriction sites downstream of a Renilla luciferase reporter, and then cloned into the psiCHECK2 dual-luciferase reporter vector (Promega, Madison, WI, USA) downstream of the Renilla luciferase reporter gene using the primers available in Supplementary Information.

**Cells culture and induction of adipocyte lineage commitment/differentiation.** C3H10T1/2 MSCs were propagated and differentiated as described previously.<sup>31</sup> C3H10T1/2 cells were cultured in DMEM (GIBCO-BRL) supplemented with 450 mg/dl glucose and 10% calf serum (PAA) and maintained at 37 °C in a 10% CO<sub>2</sub> environment. Initially, cells were seeded at a low density and allowed to grow until the following day when they were 20–30% confluent. The cells were then treated with or without BMP4 (R&D Systems, Minneapolis, MN, USA) for another 6 days in order to induce adipocyte lineage commitment. After establishing of cell commitment, the cells were then induced to differentiate in DMEM containing 10% fetal bovine serum (FBS), 1 μg/ml insulin (I), 1 μM dexamethasone (D), and 0.5 mM 3-isobutyl-1-methylxanthine (M) for 2 days; followed by incubation in DMEM containing 10% FBS and 1 μg/ml insulin for another 2 days. Cells were finally cultured in DMEM with 10% FBS.

**RNA interference.** Stealth siRNA duplexes specific to *Adams1* were designed and synthesized by Invitrogen (Carlsbad, CA, USA). The silencing effects of several siRNA duplexes were screened and tested initially by Western blot to confirm their ability to knockdown target gene expression. Stealth siRNA Negative Control Duplexes with a similar GC content were used as a control. C3H10T1/2 stem cells were transfected at 30–50% confluence with siRNA duplexes using Lipofectamine RNAi MAX (Invitrogen) according to the manufacturer's instructions.

**Western blot analyses.** Adipose tissue and cultured cells were scraped into lysis buffer containing 50 mM Tris-HCl (pH 6.8), 2% SDS, phosphatase inhibitors (10 mM Na<sub>3</sub>VO<sub>4</sub>, 10 mM NaF), and a protease inhibitor cocktail (Roche, Mannheim, Germany). Equal amounts of protein were subjected to SDS/PAGE and immunoblotted with specific primary antibodies against one of the following targets: *Adams1* (Millipore, Billerica, MA, USA); Hsp90, PPARγ, or C/EBPα, (Santa Cruz, CA, USA); 422/aP2 (prepared in Dr. Lane's lab); p38 MAPK kinase, phospho-p38, Smad1, phospho-Smad1/5/8, FAK, phospho-FAK, ERK1/2, and phospho-ERK1/2 (Cell Signaling Technology, Danvers, MA, USA); Pref1 (Proteintech Group, Chicago, IL, USA); Col5α1 (ABclonal, Cambridge, MA, USA); Thbs1 (Novus, Littleton, CO, USA); Fibronectin (BD, Franklin Lakes, NJ, USA); Col1α1 and β-actin (Sigma-Aldrich).

**Quantitative RT-PCR analysis.** Total RNA was harvested from cells or mouse adipose tissue using TRIzol reagent (Invitrogen). First strand cDNA synthesis was performed using the PrimeScript RT Master Mix (Takara Bio, Otsu, Japan) and random primers. Real-time quantitative PCR reactions were performed on an Applied Biosystems 7500 or 7900 Real-Time PCR System using the 2 × Power SYBR Green PCR Master Mix (Applied Biosystems, Carlsbad, CA, USA). The threshold cycles (Ct) for the target genes and the 18S rRNA were determined in triplicate experiments, and the relative RNA quantity was calculated using the comparative Ct method. qRT-PCR primers were available in Supplementary Information.

MiRNAs were reverse-transcribed using the TaqMan miRNA reverse transcription kit (Applied Biosystems) and miRNA-specific primers (Applied Biosystems). MiRNA expression levels were then analyzed using the TaqMan MicroRNA assay (Applied Biosystems) according to the manufacturer's instructions. Quantitation of a ubiquitously expressed miRNA (U6) was performed as an endogenous control.

**Oil red O staining.** Cells were washed three times with PBS and then fixed for 15 min with 3.7% formaldehyde. Oil Red O (0.5% in isopropanol) was diluted with water (3 : 2), filtered through a 0.45 μm filter, and then incubated with the fixed cells for 1 h at room temperature. Cells were then washed with water and the stained lipid droplets in the adipocytes were visualized by light microscopy and photographed.

**Luciferase assay.** 293T cells were plated in reduced serum and antibiotic-free Opti-MEM I and 24 h later were transfected with 10 ng of psiCHECK2-*Adams1* 3'-UTR vector and psiCHECK2-mutant *Adams1* 3'-UTR vector 24 h using Lipofectamine2000. Cells were co-transfected with either a miR-181d mimic or a negative control (Applied Biosystems) at 100 nM. After incubation for 48 h, Firefly and Renilla luciferases were measured in cell lysates using the Dual-Luciferase Reporter Assay System (Promega). Firefly luciferase activity was used for normalization and as an internal control for transfection efficiency.

**H&E staining and cell size quantification.** Standard H&E staining was performed on 5 μm thick paraffin sections of inguinal adipose tissue. Cell diameter was measured in the H&E-stained sections from 5 individual samples per group using Image J (National Institutes of Health, Bethesda, MD, USA).

**Glucose and insulin tolerance tests.** For glucose tolerance, mice were injected i.p. with D-glucose (2 mg/g body weight) after an overnight fast, and tail blood glucose levels were monitored. For insulin tolerance, mice fed ad libitum were injected i.p. with human insulin (Eli Lilly; 0.75 mU/g body weight) after a 4 h fast, and tail blood glucose levels were monitored.

**Measurements of blood parameters.** Mice blood samples were collected by retroorbital bleeding methods. Sera were prepared and used for measurements. Total cholesterol and LDL-C levels were determined using the Roche Cobas C311 chemistry analyzer.

**Adenoviral expression vectors and infection.** The adenoviral expression vector pBlock-it (Invitrogen) encoding shRNA against the *Adamts1* gene was constructed according to the manufacturer's protocols. The *Adamts1* shRNA sequence was 5'-GCCAGCAGCTACATCTGAAGT-3', and the LacZ shRNA sequence was 5'-AATTTAACCGCCAGTCAGGCT-3'. Adenovirus was amplified and purified using Sartorius Adenovirus Purification Kits (Sartorius, Goettingen, Germany). Adenovirus solution was injected subcutaneously adjacent to the mouse inguinal fat pad twice weekly for 4 weeks beginning at 6 weeks of age.

**Statistical analyses.** A non-paired Student *t*-tests were used for data analyses, and paired *t*-tests were used to compare adeno-LacZ shRNA baseline and adeno-*Adamts1* shRNA results in the same experimental mouse. Pearson's correlation analysis was used to describe the linear association between variables. The distributions of the variables of interest were examined using quantile-quantile plots. When the data were non-normally distributed, natural logarithm transformations were used to attain approximate normality before analysis. All data from samples were expressed as the mean  $\pm$  S.E.M. *P* < 0.05 was regarded as statistically significant.

### Conflict of Interest

The authors declare no conflict of interest.

**Acknowledgements.** The patients' samples of adipose tissue were kindly provided by Weiping Jia and Cheng Hu from Shanghai Jiaotong University Affiliated Sixth People's Hospital. This research was partially supported by National Key Basic Research Project Grant 2011CB910201, the State Key Program of National Natural Science Foundation 3100048C120114, and National Natural Science Foundation 81390350 (to QQ Tang.); by National Natural Science Foundation Grant 31271489 and 81170781 (to HY Huang.); by the Joint Research Fund for Overseas, Hong Kong and Macao Young Scholars (3132801) and the NIDDK-funded Minnesota Obesity Center (P30DK050456); by National Natural Science Foundation of China Grant J1210041 (to RZ Qian.). The department of biochemistry is supported by Shanghai Leading Academic Discipline Project, Project Number: B110 and by 985 Project 985III-YFX0302.

1. Sun K, Tordjman J, Clement K, Scherer PE. Fibrosis and adipose tissue dysfunction. *Cell Metab* 2013; **18**: 470–477.
2. Lijnen HR. Angiogenesis and obesity. *Cardiovasc Res* 2008; **78**: 286–293.
3. Shoelson SE, Herrero L, Naaz A. Obesity, inflammation, and insulin resistance. *Gastroenterology* 2007; **132**: 2169–2180.
4. Mariman EC, Wang P. Adipocyte extracellular matrix composition, dynamics and role in obesity. *Cell Mol Life Sci* 2010; **67**: 1277–1292.
5. Ricard-Blum S. The collagen family. *Cold Spring Harb Perspect Biol* 2011; **3**: a004978.
6. Divoux A, Tordjman J, Lacasa D, Veyrie N, Hugol D, Aissat A et al. Fibrosis in human adipose tissue: composition, distribution, and link with lipid metabolism and fat mass loss. *Diabetes* 2010; **59**: 2817–2825.
7. Henegar C, Tordjman J, Achard V, Lacasa D, Cremer I, Guerre-Millo M et al. Adipose tissue transcriptomic signature highlights the pathological relevance of extracellular matrix in human obesity. *Genome Biol* 2008; **9**: R14.
8. Varma V, Yao-Borengasser A, Bodles AM, Rasouli N, Phanavanh B, Nolen GT et al. Thrombospondin-1 is an adipokine associated with obesity, adipose inflammation, and insulin resistance. *Diabetes* 2008; **57**: 432–439.
9. Kong P, Gonzalez-Quesada C, Li N, Cavalera M, Lee DW, Frangogiannis NG. Thrombospondin-1 regulates adiposity and metabolic dysfunction in diet-induced obesity enhancing adipose inflammation and stimulating adipocyte proliferation. *Am J Physiol Endocrinol Metab* 2013; **305**: E439–E450.
10. Mori S, Kiuchi S, Ouchi A, Hase T, Murase T. Characteristic expression of extracellular matrix in subcutaneous adipose tissue development and adipogenesis; comparison with visceral adipose tissue. *Int J Biol Sci* 2014; **10**: 825–833.
11. Bolton K, Segal D, McMillan J, Jowett J, Heilbronn L, Abberton K et al. Decorin is a secreted protein associated with obesity and type 2 diabetes. *Int J Obes (Lond)* 2008; **32**: 1113–1121.
12. Kiefer FW, Zeyda M, Todoric J, Huber J, Geyeregger R, Weichhart T et al. Osteopontin expression in human and murine obesity: extensive local up-regulation in adipose tissue but minimal systemic alterations. *Endocrinology* 2008; **149**: 1350–1357.
13. Kos K, Wong S, Tan B, Gummeson A, Jernas M, Franck N et al. Regulation of the fibrosis and angiogenesis promoter SPARC/osteonectin in human adipose tissue by weight change, leptin, insulin, and glucose. *Diabetes* 2009; **58**: 1780–1788.
14. Christiaens V, Lijnen HR. Role of the fibrinolytic and matrix metalloproteinase systems in development of adipose tissue. *Arch Physiol Biochem* 2006; **112**: 254–259.

15. Lijnen HR, Maquoi E, Hansen LB, Van Hoef B, Frederix L, Collen D. Matrix metalloproteinase inhibition impairs adipose tissue development in mice. *Arterioscler Thromb Vasc Biol* 2002; **22**: 374–379.
16. Kuno K, Terashima Y, Matsushima K. ADAMTS-1 is an active metalloproteinase associated with the extracellular matrix. *J Biol Chem* 1999; **274**: 18821–18826.
17. Tang BL, Hong W. ADAMTS: a novel family of proteases with an ADAM protease domain and thrombospondin 1 repeats. *FEBS Lett* 1999; **445**: 223–225.
18. Rodriguez-Manzaneque JC, Milchanowski AB, Dufour EK, Leduc R, Iruela-Arispe ML. Characterization of METH-1/ADAMTS1 processing reveals two distinct active forms. *J Biol Chem* 2000; **275**: 33471–33479.
19. Kuno K, Okada Y, Kawashima H, Nakamura H, Miyasaka M, Ohno H et al. ADAMTS-1 cleaves a cartilage proteoglycan, aggrecan. *FEBS Lett* 2000; **478**: 241–245.
20. Lee NV, Sato M, Annis DS, Loo JA, Wu L, Mosher DF et al. ADAMTS1 mediates the release of antiangiogenic polypeptides from TSP1 and 2. *EMBO J* 2006; **25**: 5270–5283.
21. Rodriguez-Manzaneque JC, Carpizo D, Plaza-Calonge Mdel C, Torres-Collado AX, Thai SN, Simons M et al. Cleavage of syndecan-4 by ADAMTS1 provokes defects in adhesion. *Int J Biochem Cell Biol* 2009; **41**: 800–810.
22. Russell DL, Doyle KM, Ochsner SA, Sandy JD, Richards JS. Processing and localization of ADAMTS-1 and proteolytic cleavage of versican during cumulus matrix expansion and ovulation. *J Biol Chem* 2003; **278**: 42330–42339.
23. Esselens C, Malapeira J, Colome N, Casal C, Rodriguez-Manzaneque JC, Canals F et al. The cleavage of semaphorin 3C induced by ADAMTS1 promotes cell migration. *J Biol Chem* 2010; **285**: 2463–2473.
24. Vazquez F, Hastings G, Ortega MA, Lane TF, Oikemus S, Lombardo M et al. METH-1, a human ortholog of ADAMTS-1, and METH-2 are members of a new family of proteins with angio-inhibitory activity. *J Biol Chem* 1999; **274**: 23349–23357.
25. Luque A, Carpizo DR, Iruela-Arispe ML. ADAMTS1/METH1 inhibits endothelial cell proliferation by direct binding and sequestration of VEGF165. *J Biol Chem* 2003; **278**: 23656–23665.
26. Kuno K, Kanada N, Nakashima E, Fujiki F, Ichimura F, Matsushima K. Molecular cloning of a gene encoding a new type of metalloproteinase-disintegrin family protein with thrombospondin motifs as an inflammation associated gene. *J Biol Chem* 1997; **272**: 556–562.
27. Bourd-Boittin K, Bonnier D, Leyme A, Mari B, Tuffery P, Samson M et al. Protease profiling of liver fibrosis reveals the ADAM metalloproteinase with thrombospondin type 1 motif, 1 as a central activator of transforming growth factor beta. *Hepatology* 2011; **54**: 2173–2184.
28. Shindo T, Kurihara H, Kuno K, Yokoyama H, Wada T, Kurihara Y et al. ADAMTS-1: a metalloproteinase-disintegrin essential for normal growth, fertility, and organ morphology and function. *J Clin Invest* 2000; **105**: 1345–1352.
29. Tan Ide A, Ricciardelli C, Russell DL. The metalloproteinase ADAMTS1: a comprehensive review of its role in tumorigenic and metastatic pathways. *Int J Cancer* 2013; **133**: 2263–2276.
30. Thai SN, Iruela-Arispe ML. Expression of ADAMTS1 during murine development. *Mech Dev* 2002; **115**: 181–185.
31. Tang QQ, Otto TC, Lane MD. Commitment of C3H10T1/2 pluripotent stem cells to the adipocyte lineage. *Proc Natl Acad Sci USA* 2004; **101**: 9607–9611.
32. Qian SW, Tang Y, Li X, Liu Y, Zhang YY, Huang HY et al. BMP4-mediated brown fat-like changes in white adipose tissue alter glucose and energy homeostasis. *Proc Natl Acad Sci USA* 2013; **110**: E798–E807.
33. Huang H, Song TJ, Li X, Hu L, He Q, Liu M et al. BMP signaling pathway is required for commitment of C3H10T1/2 pluripotent stem cells to the adipocyte lineage. *Proc Natl Acad Sci USA* 2009; **106**: 12670–12675.
34. Volloch V, Olsen BR. Why cellular stress suppresses adipogenesis in skeletal tissue, but is ineffective in adipose tissue: control of mesenchymal cell differentiation via integrin binding sites in extracellular matrices. *Matrix Biol* 2013; **32**: 365–371.
35. Schaller MD. Biochemical signals and biological responses elicited by the focal adhesion kinase. *Biochim Biophys Acta* 2001; **1540**: 1–21.
36. Schlaepfer DD, Hanks SK, Hunter T, van der Geer P. Integrin-mediated signal transduction linked to Ras pathway by GRB2 binding to focal adhesion kinase. *Nature* 1994; **372**: 786–791.
37. Hatipoglu OF, Hirohata S, Yaykasli KO, Cilek MZ, Demircan K, Shinohara R et al. The 3'-untranslated region of ADAMTS1 regulates its mRNA stability. *Acta Med Okayama* 2009; **63**: 79–85.
38. Divoux A, Clement K. Architecture and the extracellular matrix: the still unappreciated components of the adipose tissue. *Obes Rev* 2011; **12**: e494–e503.
39. Labat-Robert J. Cell-matrix interactions, the role of fibronectin and integrins. A survey. *Pathol Biol (Paris)* 2012; **60**: 15–19.
40. Roy DC, Hocking DC. Recombinant fibronectin matrix mimetics specify integrin adhesion and extracellular matrix assembly. *Tissue Eng A* 2013; **19**: 558–570.
41. Maquoi E, Munaut C, Colige A, Collen D, Lijnen HR. Modulation of adipose tissue expression of murine matrix metalloproteinases and their tissue inhibitors with obesity. *Diabetes* 2002; **51**: 1093–1101.
42. Nie J, Sage EH. SPARC inhibits adipogenesis by its enhancement of beta-catenin signaling. *J Biol Chem* 2009; **284**: 1279–1290.
43. Nie J, Sage EH. SPARC functions as an inhibitor of adipogenesis. *J Cell Commun Signal* 2009; **3**: 247–254.

44. Matthews BD, Overby DR, Mannix R, Ingber DE. Cellular adaptation to mechanical stress: role of integrins, Rho, cytoskeletal tension and mechanosensitive ion channels. *J Cell Sci* 2006; **119**: 508–518.
45. Huang HY, Zhang WT, Jiang WY, Chen SZ, Liu Y, Ge X *et al*. RhoGDIbeta inhibits BMP4-induced adipocyte lineage commitment and favors smooth muscle-like cell differentiation. *J Biol Chem* 2015; **290**: 11119–11129.
46. Li Z, Fei T, Zhang J, Zhu G, Wang L, Lu D *et al*. BMP4 Signaling Acts via dual-specificity phosphatase 9 to control ERK activity in mouse embryonic stem cells. *Cell Stem Cell* 2012; **10**: 171–182.
47. Ambros V. The functions of animal microRNAs. *Nature* 2004; **431**: 350–355.
48. Ma J, Jiang Z, He S, Liu Y, Chen L, Long K *et al*. Intrinsic features in microRNA transcriptomes link porcine visceral rather than subcutaneous adipose tissues to metabolic risk. *PLoS One* 2013; **8**: e80041.
49. Hulsmans M, Sinnaeve P, Van der Schueren B, Mathieu C, Janssens S, Holvoet P. Decreased miR-181a expression in monocytes of obese patients is associated with the occurrence of metabolic syndrome and coronary artery disease. *J Clin Endocrinol Metab* 2012; **97**: E1213–E1218.
50. Li H, Chen X, Guan L, Qi Q, Shu G, Jiang Q *et al*. MiRNA-181a regulates adipogenesis by targeting tumor necrosis factor-alpha (TNF-alpha) in the porcine model. *PLoS One* 2013; **8**: e71568.
51. Zhou B, Li C, Qi W, Zhang Y, Zhang F, Wu JX *et al*. Downregulation of miR-181a upregulates sirtuin-1 (SIRT1) and improves hepatic insulin sensitivity. *Diabetologia* 2012; **55**: 2032–2043.
52. Whittaker R, Loy PA, Sisman E, Suyama E, Aza-Blanc P, Ingermanson RS *et al*. Identification of MicroRNAs that control lipid droplet formation and growth in hepatocytes via high-content screening. *J Biomol Screen* 2010; **15**: 798–805.

Supplementary Information accompanies this paper on Cell Death and Differentiation website (<http://www.nature.com/cdd>)